Influence of homolog composition and hydration states of magnesium stearate on carrier-based dry powder formulations for inhalation

Tingting Liu , Wenwen Xu , Xiaoxiao Gao , Li Pan , Maosheng Cheng , Baoming Ning , Jukka Rantanen , Dongmei Cun , Mingshi Yang

PII: S0928-0987(25)00348-3
DOI: https://doi.org/10.1016/j.ejps.2025.107351
Reference: PHASCI 107351

To appear in: *European Journal of Pharmaceutical Sciences*

Received date: 29 August 2025
Revised date: 23 October 2025
Accepted date: 24 October 2025

Please cite this article as: Tingting Liu , Wenwen Xu , Xiaoxiao Gao , Li Pan , Maosheng Cheng , Baoming Ning , Jukka Rantanen , Dongmei Cun , Mingshi Yang , Influence of homolog composition and hydration states of magnesium stearate on carrier-based dry powder formulations for inhalation, *European Journal of Pharmaceutical Sciences* (2025), doi: https://doi.org/10.1016/j.ejps.2025.107351

Influence of homolog composition and hydration states of magnesium stearate on carrier-based dry powder formulations for inhalation

Tingting Liu[1,2,3], Wenwen Xu[1,4], Xiaoxiao Gao[1], Li Pan[5], Maosheng Cheng[5], Baoming Ning[2,3], Jukka Rantanen[6], Dongmei Cun[7], Mingshi Yang[1,4,6*]

[1]Wuya College of Innovation, Shenyang Pharmaceutical University, No. 103, Wenhua Road, 110016 Shenyang, China

[2]National Institutes for Food and Drug Control (NIFDC), No. 31, Huatuo Road, Daxing District, Beijing 102629, China

[3]State Key Laboratory of Drug Regulatory Science, Beijing, 102629, China

[4]Joint International Research Laboratory of Intelligent Drug Delivery Systems, Ministry of Education, 110016, Shenyang, China

[5]Department of Medicinal Chemistry, School of Pharmaceutical Engineering, Shenyang Pharmaceutical University, Wenhua Road No. 103, 110016 Shenyang, China

[6]Department of Pharmacy, University of Copenhagen, Universitetsparken 2, DK-2100 Copenhagen, Denmark

[7]School of Food and Drug, Shenzhen Polytechnic University, China, Shenzhen 518055, China

* Corresponding author.

E-mail: mingshi.yang@sund.ku.dk

Tel: 0045 35 33 61 41

Abstract

Magnesium stearate (MgSt) has been used as a force control agent (FCA) to enhance the aerosol performance of carrier-based dry-powder inhalers (DPIs). MgSt is a mixture of magnesium salts of fatty acids—primarily stearic acid (SA) and palmitic acid (PA)—and the SA:PA ratio can vary depending on the natural source. In addition, different processing routes can yield variation in both chemical and solid form composition of commercial grade MgSt. This study investigated whether variations in fatty acid composition and hydration state (hydrate form) of MgSt affect the aerosol performance of carrier-based DPIs. Samples of MgSt with different SA/PA molar ratios and hydration states were obtained and micronized, then blended with coarse lactose (carrier) and tratinterol hydrochloride (TH), a new long-acting bronchodilator used as a model drug, to prepare DPI formulations (TH-DPIs). After physicochemical characterization, the aerosol

performance of the TH-DPI formulations was assessed using a Next Generation Impactor (NGI). NGI results showed that the fine particle fraction (FPF) of TH-DPIs increased with increasing MgSt content, irrespective of fatty acid composition or hydration state. Changes in the SA/PA ratio had little effect on aerosol performance. In contrast, formulations containing trihydrate MgSt generally exhibited higher FPFs than those containing dihydrate or low-hydration MgSt. In conclusion, changes in the hydration state of MgSt exert a greater impact on DPI aerosol performance than variations in its fatty-acid composition.

Key words: dry powder inhaler; magnesium stearate; hydration state; homolog composition; water sorption; surface energy

1. Introduction

In recent years, dry powder inhaler (DPI) formulations are well established for the treatment of pulmonary diseases (Boer et al., 2017). Most of DPIs are composed of coarse lactose particles as carriers (> 50 μm) and micronized drug particles (< 5 μm), in which the carriers prevent the aggregation of drug particles, increase the powder bulk and improve the flowability (Ooi et al., 2011). However, some studies have shown that the excessive adhesion between the carrier particles and drug particles confines the separation of the drug from the carriers, which is the main factor leading to the low efficiency of drug delivery (Begat et al., 2004; Pilcer et al., 2012; Xian et al., 2000). To overcome this challenge, different methods have been attempted to reduce the strong interaction between micronized drug fine particles and the carriers, in which an addition of force control agent (FCA) in DPIs is considered to be an effective method (Peng et al., 2016). As one of the FCAs, magnesium stearate (MgSt) is well-known for the improvement of aerodynamic performance of carrier-based DPIs (Begat et al., 2005; Jetzer et al., 2017). It has been used in some Food and Drug Administration (FDA) approved DPI products, such as Foradil Certihaler® and Breo Ellipta® (1% in vilanterol dry powder) to improve the lung deposition efficiency of the active pharmaceutical ingredients. Our recent study also showed that MgSt is capable of improving lung deposition of tratinterol hydrochloride (TH), a new long-acting bronchodilator with strong β2 adrenoceptor stimulation activity by formulating them into carrier-based DPIs (Liu et al., 2022). That study also showed that, compared to MgSt as received, fine particle fraction (FPF) of TH could be improved further when it was formulated with micronized MgSt (Liu et al., 2022).

Even though there are many papers reporting the FCA role of MgSt (Guchardi et al., 2008; Lau et al.,

2017; Peng et al., 2016; Zhou et al., 2012), the exact mechanisms behind improving aerosol performance of DPI by this excipient have not been fully understood. It is generally believed that MgSt can coat the surface of the coarse lactose particles as carriers upon the mixing process involved in the preparation of dry powders for inhalation. The lipophilic carbon chains of MgSt are aligned outward, which consequently reduces the strong binding of drug particles to the lactose carrier. As a result the fine drug particles can readily detach from the carrier and result in enhanced lung deposition during inhalation. However, there was no quantitative analysis of the modifying effect of MgSt. Moreover, MgSt is a mixture of magnesium salts of fatty acids — primarily stearic acid (SA) and palmitic acid (PA). These fatty acids are commonly found together in natural sources (like animal fats or vegetable oils), which are used in the industrial production of MgSt. Commercial MgSt often contains both magnesium stearate and magnesium palmitate. The SA/PA ratio depends on the source of the fatty acids and the manufacturing process and purification steps.

In addition, MgSt can possess multiple hydration states (hydrate forms): anhydrate, monohydrate, dihydrate and trihydrate (Delaney et al., 2017). MgSt can exist as dominantly single hydration state system, or contain multiple hydration states (Swaminathan and Kildsig, 2001). The impact of this variation has been thoroughly investigated for tablet manufacturing processes, as exemplified by Calahan et al. (Calahan et al., 2020). However, the studies on how different hydration states of MgSt affecting aerosol performance of DPIs are limited, although a recent study reported that the monohydrate form of magnesium stearate improved the DPI performance of arformoterol and budesonide more effectively than the anhydrate or dihydrate form (Jeong et al., 2025). Interestingly, trihydrate form of MgSt was not included in the study. It should be noted that crystal structures of commercial MgSt hydrate forms have not yet been published, despite the efforts to characterize, e.g., the pure magnesium stearate hydrate forms(Herzberg et al., 2023).

Tratinterol hydrochloride (TH; 2-(3-chloro-4-amino-5-trifluoromethyl-phenyl)-2-tert-butanol • HCl) is a novel, long-acting β_2-adrenergic receptor agonist (LABA) that displays high receptor selectivity. A phase-III oral-dose trial showed TH to be as effective and well tolerated as procaterol hydrochloride tablets (Kong et al., 2021). Our previous work has additionally demonstrated the feasibility of formulating TH as a dry-powder inhaler (Liu et al., 2023).

This study aimed to investigate whether the variation in the SA/PA ratio and the hydration states including trihydrate form of MgSt would influence the aerosol performance of DPIs of TH, a new long-acting bronchodilator. To this end, we prepared various MgSt with different SA/PA ratios and hydration states prior to modifying coarse lactose particles with these MgSt. TH was used as a model drug to prepare carrier-based

DPIs in this study. The effect of various MgSt on the aerosol performance of TH-DPIs was assessed using next generation pharmaceutical impactor.

2. Materials and methods

2.1. Materials

Coarse lactose (Lactohale® 206, α-lactose monohydrate,) was donated by DFE pharma. Tratinterol hydrochloride (TH) was supplied by Jinzhou Jiutai Co., Ltd, the micronized TH fine powders was described in our previous study (Liu et al., 2023). MgSt (SH-YM-M) was provided by Anhui Sunhere Pharmaceutical Excipients Co., Ltd. Stearic acid and palmitic acid (purity >97%) was obtained from Shanghai Macklin Biochemical Technology Co., Ltd. Sodium hydroxide, magnesium chloride hexahydrate, acetone and Twain 80 of chemical grade, and all other chemicals and solvents of HPLC grade were purchased from Shandong Yuwang Pharmaceutical Co., Ltd. #3 hydroxypropyl methyl cellulose (HPMC) capsule was a gift from Capsugel Co., Ltd. Purified water was obtained from Milli-Q water machine.

2.2. Synthesis of magnesium stearate and magnesium palmitate

MgSt samples were synthesized by dispersing combinations of SA and PA (100/0, 50/50 and 0/100) in 3 liters of Milli-Q water previously heated to 90°C. Sodium hydroxide solution (40.0 N) was added dropwise until the solution reached a pH of 9.7, generating a fatty acid soap with SA and/or PA. MgSt was precipitated out of the solution by the addition of a stoichiometric excess of $MgCl_2 \cdot 6H_2O$. Finally, magnesium stearate composed of pure SA (i.e. SA/PA:100/0, denoted as MgSt-S), magnesium stearate composed of 50% of SA and 50% of PA (i.e. SA/PA:50/50, denoted as MgSt-SP,) and magnesium stearate composed of 100% of PA (i.e. SA/PA:0/100, denoted as MgSt-P) were isolated by vacuum filtration and were washed with acetone and water for 24 hours, respectively. It should be noted that the abbreviation MgSt-P can be confusing, but it is considered that in the context of this study this abbreviation is justified.

To exclude the influence of particle size on the results, MgSt-S, MgSt-SP and MgSt-P were micronized using jet mill (MC-20, Micromacinazione®, Sweden). Nitrogen was used as the milling gas. The grinding pressure of 6.0 bar and injector pressure of 7.0 bar has been found optimal and the feed rate was kept constant at 0.5 g/min. The products were defined as MgSt-MS, MgSt-MSP and MgSt-MP, respectively.

2.3. Production of magnesium stearate with different hydration state

Commercial MgSt (MgSt-C) as received were micronized using the procedure reported previously (Liu et al., 2022), denoted as MgSt-MC. To lower hydration state of MgSt, MgSt-MC was placed in a 80℃ of vacuum oven for 48 hours to obtain MgSt-ML (micronized MgSt with low hydration state). To increase the hydration state in MgSt samples MgSt-ML was placed in an artificial climate chamber (QHX-205BSH-Ⅲ, Cimo Medical Instrument Co.,LTD, China) with a relative humidity of 90% at 25℃ for 72 hours to obtain MgSt-MH (micronized MgSt with high hydration state).

2.4. Modification of coarse lactose carrier and preparation of TH-DPIs formulation

Prior to preparation of TH-DPIs, coarse lactose were modified by blending them with various concentrations (0.25%, 0.5%, 0.75% and 1%, w/w) of micronized MgSt using a high shear mixer (Mini-G, 1L, Shenzhen Xinyite Science and Technology Co., Ltd.) at the impeller speed of 300 rpm for 30 min. The modified lactose particles were named as MLac. Subsequently, TH-DPIs were prepared by mixing the MLac lactose with micronized TH fine powders using the same high shear mixer at the impeller speed of 200 rpm for 20 min. The final contraction of TH in the formulations is 0.13% (w/w). The obtained TH-DPIs and modified coarse lactose carriers were packed in aluminum bags and then stored at room temperature (between 15 ℃ and 25 ℃, with relative humidity below 60 %) prior to further analysis. A summary of the TH-DPIs is summarized in Table 1.

Table 1 The composition of TH-DPIs.

Formulations	Modified lactose	MgSt type	MgSt (%, w / w)
TH-DPI-S	MLac-MS	MgSt-MS	0.25, 0.50, 0.75, 1.00
TH-DPI-SP	MLac-MSP	MgSt-MSP	0.25, 0.50, 0.75, 1.00
TH-DPI-P	MLac-MP	MgSt-MP	0.25, 0.50, 0.75, 1.00
TH-DPI-L	MLac-ML	MgSt-ML	0.25, 0.50, 0.75, 1.00
TH-DPI-C	MLac-MC	MgSt-MC	0.25, 0.50, 0.75, 1.00
TH-DPI-H	MLac-MH	MgSt-MH	0.25, 0.50, 0.75, 1.00

2.5. Particle size and distribution

Particle size and distributions of initial and processed MgSt were determined using a Sympatec HELOS/RODOS (Sympatec GmbH, Clausthal-Zellerfeld, Germany) employing a vibratory feeder, and a R1 lens with a measuring range of 0.18 μm to 35 μm. The dispersive pressure was set up as 4.0 bar. PSDs (D_{10}, D_{50} and D_{90}) were calculated using Fraunhofer theory and analyzed in WINDOX 4.0 software (Sympatec

GmbH, Clausthal-Zellerfeld, Germany) and the Span value defined as $(D_{90}-D_{10})/D_{50}$.

Particle size and distributions of coarse lactose were carried out using a BT-9300LD dry method (Bettersize, Dandong, China) with a vibratory feeder, and the measuring range of 0.1 μm to 1036 μm. The evaluation of raw data was analyzed using the Better particle size analyzer (Bettersize, Dandong, China).

2.6. Particle morphology

The morphology of MgSt and MgSt micro-powder was observed using a scanning electron microscope (SEM, Supra 35, Zeiss, Oberkochen, Germany). The samples were mounted on an aluminum plate using conductive carbon tape, then coated with thin gold films using a sputtering coater under vacuum. The samples were then observed under the SEM with an accelerating voltage of 10 kV.

2.7. Thermal analyses

2.7.1 Differential scanning calorimetry (DSC)

DSC thermograms (DSC-1, Mettler Toledo, Switzerland) were obtained under a nitrogen gas flow of 40 mL/min. Sample powders (3 to 5 mg) were filled into a pin-holed hermetically sealed aluminum pan and weighed. The samples were then heated from 25 °C to 200 °C at a scanning rate of 10 °C/min.

2.7.2 Thermo gravimetric analysis (TGA)

A TGA system (TGA550, TA Instruments, America) was used for investigation of the hydration state, of the MgSt samples. Samples of about 3 mg were placed in an open alumina pan. Nitrogen was used as the purge gas at a flow of 40 mL/min. The heating cycle was from 25℃ to 200℃ at a scanning rate of 10 °C/min. The total weight loss from room temperature to 125℃ was analyzed for the water content of MgSt samples.

2.8. X-ray powder diffraction (XRPD)

The hydrate forms of MgSt samples were also investigated using an XRPD (DX-2700, Dandong Fangyuan Co., Ltd., China) with a CuK α X-ray source (λ = 1.54 Å) generated at 300 mA and 40 kV. The diffraction patterns of samples were collected from a 2θ of 5° to 45° at the rate of 15°/min and a step size of 0.05°.

2.9. Aerodynamic assessment

The *in vitro* inhalation performance was evaluated by dispersing 15 mg powder into Next Generation Impactor (NGI) (Beijing Huironghe Technology Co., Ltd., China) using a low flow resistance ICOcap® inhaler at a constant air flow rate of 60 L/min for an actuation time of 4 seconds. Size 3 HPMC capsules were used for powder loading each containing 15 mg of DPI powder. To ensure detectable drug deposition on the collection plate, ten capsules were aerosolised per experiment. Every stage of NGI involved coating with Tween 80 ethanol solution (2%, w/v). After dispersion, the deposited drug in the capsule, inhaler and adaptor, throat, pre-separator, and the NGI stages was recovered by exhaustively washing with pure water and quantified using high performance liquid chromatography (HPLC) method. The emitted dose (ED) was defined as a percentage of the mass collected from the throat, pre-separator, stages 1–7 and Micro-orifice collector (MOC) relative to the total collected mass. Fine particle dose (FPD) was defined as the total mass of drug particles with an aerodynamic diameter < 5 μm. Fine particle fraction (FPF) was the FPD expressed as a percentage of the mass collected from the throat, pre-separator, stages 1–7 and MOC. Mass median aerodynamic diameter (MMAD) was the diameter at the 50% cumulative percentage, while the geometric standard deviation (GSD) was defined as a measure of the spread of the aerodynamic particle size distribution (USP, (601)).

2.10. Specific surface area (SSA) and surface energy (SE)

The specific surface area (SSA) and the surface energy (SE) of coarse lactose and MLs were carried out using the surface energy analyser (SEA, Surface Measurement Systems Ltd., UK). The samples were weighed into silanised glass columns (4 mm inner diameter) and fixed with silanised glass wool on both ends. To avoid hollows and cracks in the powder bed, the filled columns were compressed by tapping for 10 min using the SMS column packer accessory. Before each measurement, the column was conditioned at 0% relative humidity (RH) and 10 mL/min carrier gas flow (nitrogen) for one hour to get rid of any volatile contamination.

The SSA measurement were carried out using the BET principle (Brunauer et al., 1938). The conditioned sample column was injected with a series of octane injections at 30°C to obtain the adsorption isotherm. The calculation of the SSA was based on the linear section of the adsorption isotherm (p/p_0: 0.05–0.35).

The SE distribution of sample was carried out using the same column as SSA. The measurements were

conducted by injecting a series of alkanes (octane—decane) for dispersive part of SE as well as chloroform and toluene for acid-base part of SE. All injected concentrations were from 0.5% up to 20%. For the determination of the dead volume, a double injection of methane was performed at the beginning and the end of every experiment.

The raw data were analysed using the SEA Analysis Software (Surface Measurement Systems Ltd., UK). Calculations were based on the DellaVolpe scale in combination with the Dorris and Gray approach and the polarisation method. For SSA calculations, peak maxima were used, for SE calculations served the peak centre of mass.

2.11. Assay

TH concentrations were determined by a validated reversed-phase HPLC method. Analyses were performed on a HPLC system (Hitachi model Chromaster-series, Hitachi, High Technologies Chromaster, Tokyo, Japan) equipped with a model 5410 UV detector and Thermo BDS Hypersil C18 column (250 mm × 4.6 mm i.d., 5 µm). The column temperature was maintained at 40 °C and the UV detection wavelength was set at 246 nm. The mobile phase consisted of 22 % (v/v) acetonitrile and 78 % (v/v) phosphate buffer (4 mL triethylamine L^{-1}, pH 3.5 ± 0.1, adjusted with phosphoric acid) delivered at 1.0 mL min^{-1}. Sample injection volume was 20 µL. The method was linear over the range 0.05–20.0 µg mL^{-1} (r^2 = 0.999) with a limit of quantitation (LOQ) of 0.02 µg mL^{-1}.

2.12. Analysis of statistical significance

This study reports the characterization results of a single-batch sample. The experiments for each sample were performed in triplicate unless otherwise specified. The results are given as the mean value ± standard deviation (SD). The significance of differences was evaluated using one-way analysis of variance (ANOVA) and a *p* value less than 0.05 was considered as statistically significant.

3. Result and discussion

Magnesium stearate (MgSt) is a mixture of magnesium salts of fatty acids—primarily stearic acid (SA) and palmitic acid (PA). The SA:PA ratio in MgSt can vary depending on the natural source. The solid-state properties of MgSt can be considered at three levels: (i) molecular (composition and hydration state), (ii) particle (size and crystal habit), and (iii) bulk powder (density and porosity). As an FCA in DPIs, each of

these properties can affect the functional performance of MgSt. This study investigates how the fatty-acid (homologue) composition and hydration state of MgSt influence DPI performance.

3.1. Particle size distribution

In the previous study (Liu et al., 2022), we demonstrated that aerosol performance of TH-DPIs could be increased when incorporating micronized MgSt as compared to using commercial MgSt as received. In this study, to investigate the effect of fatty acid composition and hydrate state of MgSt on aerosol performance of TH-DPIs, the newly synthesized MgSt (i.e. MgSt-S, MgSt-SP, and MgSt-P) as well as those newly prepared MgSt with different hydration state were micronized using a jet mill prior to formulation using the same procedure reported in previously (Liu et al., 2022).

In Table 2, the particle size distributions of the MgSt samples are presented. Prior to micronization, the median diameter (D_{50}) of the commercial and synthetic MgSt samples are higher than 6 μm. After the jet milling process, the size of micronized MgSt decreased significantly. As shown in Table 2 the D_{50} of micronized MgSt variants are less than 2.0 μm and the span values are also decreased. It suggests that the particle size distribution became narrower post micronization. There was no significant difference among the particle size of MgSt-ML, MgSt-MC and MgSt-MH. It was further observed that the vacuum drying and humidification operations had negligible effect on the diameters of the micronized MgSt powders.

Table 2 Particle size and distribution of MgSt, TH fine powder and coarse lactose. (Mean ± SD, n = 3). Note: The data of TH fine powder and coarse lactose are from our previous study(Liu et al., 2023).

MgSt samples	Diameter (μm)			Span
	D_{10}	D_{50}	D_{90}	
MgSt-C	1.9 ± 0.0	8.9 ± 0.1	19.8 ± 0.1	2.0 ± 0.0
MgSt-S	2.0 ± 0.2	7.5 ± 0.8	16.9 ± 2.6	2.0 ± 0.1
MgSt-SP	2.0 ± 0.0	6.0 ± 0.1	12.9 ± 0.2	1.8 ± 0.0
MgSt-P	2.0 ± 0.1	6.9 ± 0.5	13.3 ± 1.7	1.7 ± 0.1
MgSt-MS	0.6 ± 0.0	1.6 ± 0.0	3.1 ± 0.0	1.5 ± 0.0
MgSt-MSP	0.8 ± 0.0	2.0 ± 0.0	3.8 ± 0.1	1.5 ± 0.0
MgSt-MP	0.6 ± 0.0	1.7 ± 0.0	3.5 ± 0.0	1.7 ± 0.0
MgSt-MC	0.7 ± 0.0	1.9 ± 0.0	3.4 ± 0.0	1.5 ± 0.0
MgSt-ML	0.7 ± 0.0	1.9 ± 0.0	3.5 ± 0.0	1.4 ± 0.0
MgSt-MH	0.7 ± 0.0	1.9 ± 0.0	3.5 ± 0.0	1.5 ± 0.0
TH fine powder*	0.5 ± 0.0	1.1 ± 0.0	2.0 ± 0.0	1.4 ± 0.0
Coarse lactose*	29.4 ± 0.3	79.9 ± 1.1	157.9 ± 6.2	1.6 ± 0.1

3.2. Morphology of MgSt samples

As shown in Figure 1, synthetic MgSt samples (i.e. MgSt-S, MgSt-SP and MgSt-P) exhibit irregular,

plate-like shapes, which is similar to the commercial MgSt as received (MgSt-C). Post micronization *via* jet milling, the sizes of synthetic MgSt particles decreased, which are in agreement with the results in Table 2. The micronized MgSt treated under different conditions, i.e. MgSt-ML, MgSt-MC, MgSt-MH did not exhibit different shape and sizes, indicating the storage of the samples in vacuum oven or artificial climate chamber with a relative humidity of 90% did not alter their morphology.

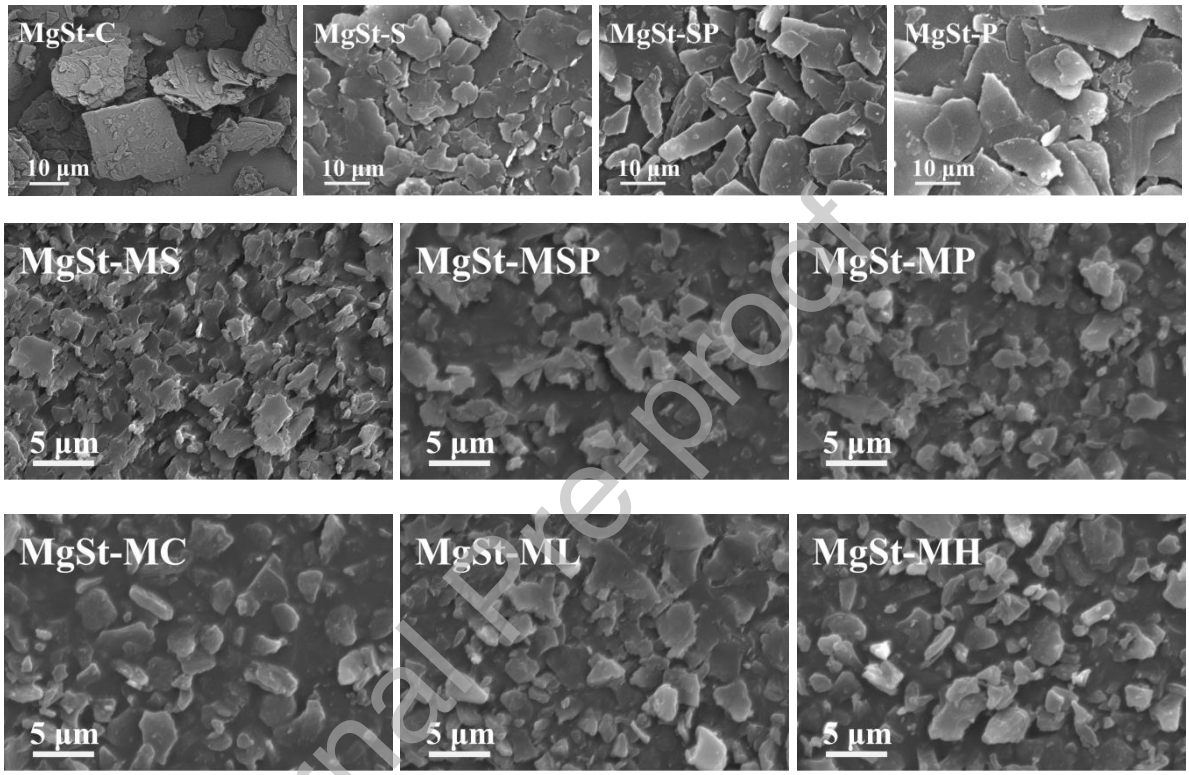

Fig.1 SEM images of MgSt samples. Note: The images of MgSt-C and MgSt-MC are from our previous study (Liu et al., 2022).

3.3. Characterization of hydration state of synthetic MgSt samples

The hydration state of MgSt samples used in this study was determined by using combined techniques, including TGA, DSC, and XRPD. As shown in Fig. 2A, all synthetic MgSt samples, i.e. MgSt-S, MgSt-SP, and MgSt-P, and their micronized samples experienced similar weight losses, i.e. 5%-6%, upon TGA experiment. As reported previously depending on the composition of the fatty acids in MgSt, H_2O accounts for about 2.9%-3.2% (monohydrate) of the weight of MgSt (Delaney et al., 2017). Therefore the loss of the mass (5%-6%) could be attributed to two molecules of H_2O (dihydrate). Due to the hydrophobic fatty acid chains present on the outermost surface of the MgSt lattice, it strongly hinders the surface adsorbed water.

Therefore, we attribute the DSC and TGA events mainly to the loss of hydrate forming water, rather than surface adsorbed water.

DSC results (Fig. 2B) show that all samples had two endothermic peaks. The thermal event around 100℃-107℃ can be assigned to the loss of water and the event around 112℃-121℃ can be assigned to the melting of the materials. As SA has two more -CH_2 than PA, the melting points of synthetic MgSt decrease with a decrease in SA in the molecular structure. The thermal analysis suggest that synthetic MgSt samples were dominantly in dihydrate forms. Seen from the XRPD patterns in Fig. 2C, all synthetic MgSt and their micronized samples (except for MgSt-P) possess diffraction peaks around 5°, 22°, and 23.6° of 2θ, which is consistent with the patterns of dihydrate MgSt reported in literature(Delaney et al., 2017). As for the XRPD pattern of MgSt-P, the diffraction peaks at 5.6°, 9.3°, 11.1°, 14.8°, and 23.3° of 2θ can be assigned to the dihydrate of pure magnesium palmitate (Ertel and Carstensen, 1988).

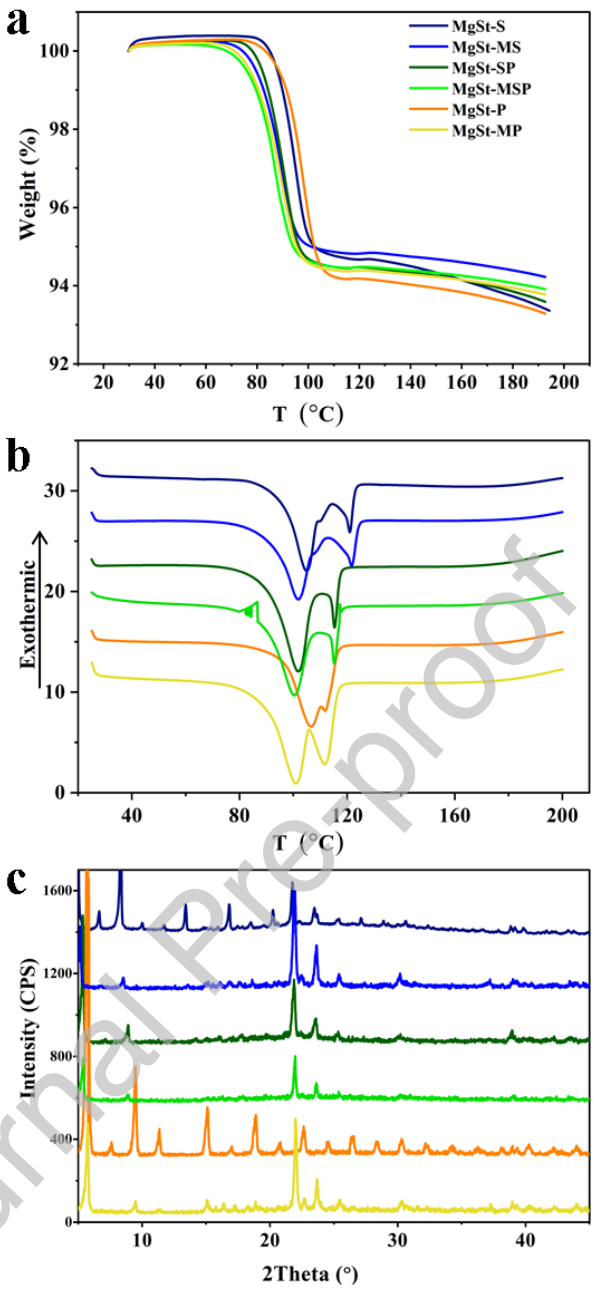

Fig. 2 The TGA weight loss plots (a), DSC thermograms (b), and XRPD patterns (c) for MgSt-S, MgSt-SP, MgSt-P, and their corresponding micronized samples, i.e. MgSt-MS, MgSt-MSP, and MgSt-MP.

3.4. Characterization of MgSt with different hydration state

As shown in Fig. 3A, the weight losses of MgSt samples in TGA measurement increase in an order of MgSt-ML (2.3%), MgSt-C (3.3%), MgSt-MC (4.4%) and MgSt-MH (7.7%), which were estimated from the weight loss between 40 – 120°C from the TGA curves. Seen from Fig. 3B, the shapes of the DSC curves of MgSt-C and MgSt-MC are similar, indicating post micronization MgSt remained dominantly as dihydrate

form. The thermal events related to the dehydration in the sample of MgSt-ML at around 90 – 100 °C is much weaker than those of MgSt-C and MgSt-MC. It suggests MgSt-ML contained the least water, which is in agreement with the TGA result. The thermal events of the dehydration in the sample of MgSt-MH at around 80 – 100 °C is much stronger than that of MgSt-C and MgSt-MC. When looking at the XRPD patterns in Fig. 3C, it can be concluded that MgSt-MH is a trihydrate with characteristic diffraction peaks at 20° 2θ and 23.5° 2θ. The XRPD patterns of MgSt-ML, MgSt-C and MgSt-MC suggest that they are dominantly dihydrate form (characteristic post micronization MgSt remained dominantly as dihydrate form.diffraction peaks are 22°, 23.6°, 39° and 40° 2θ), although both TGA and DSC results suggest that MgSt- ML contained less water than MgSt-MC in the molecules. It implies that MgSt-ML may be a mixture of MgSt dihydrate and MgSt anhydrate or monohydrate.

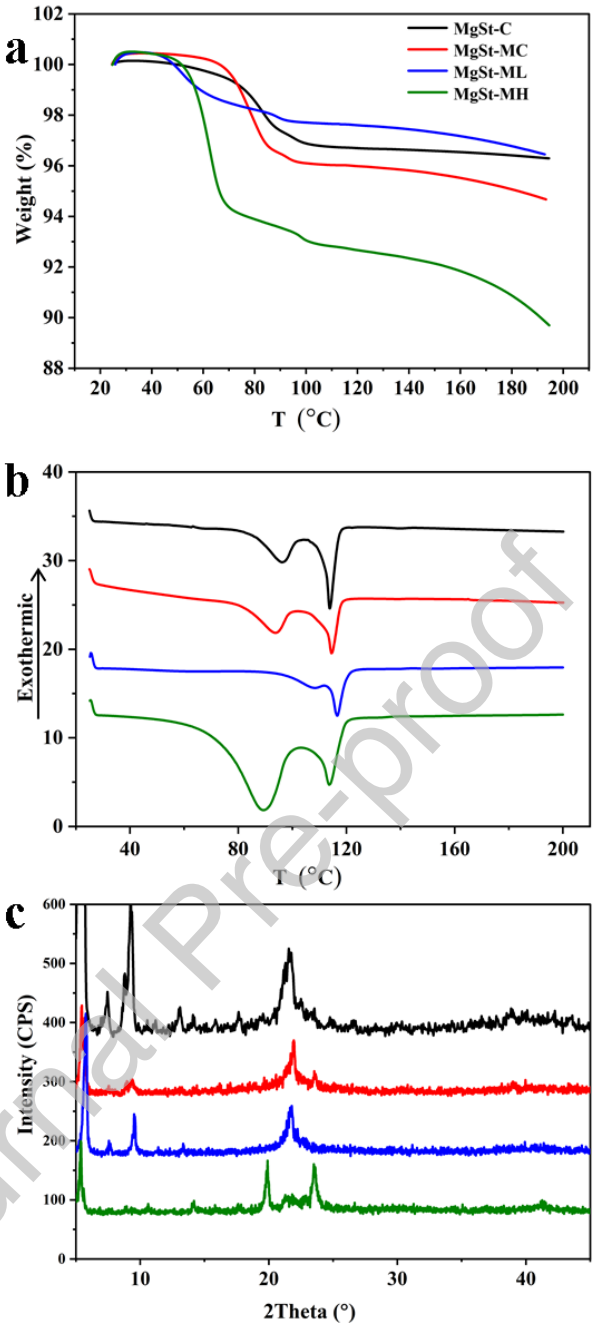

Fig. 3 The TGA weight loss plots (a), DSC thermograms (b), and XRPD patterns (c) for MgSt-C, MgSt-MC, MgSt-ML and MgSt-MH samples.

3.5. Assessment of aerodynamic characteristics of fine particles

To investigate the effect of fatty-acid (homologue) composition and hydration state of MgSt on the aerosol performance of carrier-based TH-DPIs, NGI was employed to assess the aerodynamic characteristics of the fine particles including ED, FPF, MMAD, and GSD.

3.5.1 Influence of homolog composition of MgSt on the aerodynamic characteristics

The depositions of TH-DPIs composed of MgSt with different SA/PA ratios in different parts of NGI are shown in Fig. 4. The results showed that the variations in SA/PA ratio of MgSt had similar effects on aerodynamic characteristics of the fine particles. When the proportion of MgSt increased from 0.25% to 1% (w/w) in the formulations, the residual TH in the capsules increased, the deposition of TH in the pre-separator decreased, and the deposition of TH at stage 3 to stage 7 increased.

The same trends in ED, FPF, and GSD were observed irrespective of fatty acid composition (MgSt-MS, MgSt-MSP, or MgSt-MP) as shown in Fig. 5. The EDs of the TH-DPIs decrease with an increase in the proportion of MgSt in the formulation (Fig. 5A), whereas FPFs and GSDs of TH-DPIs increase (Fig. 5B, 5D). No clear trend in the change in MMADs of the TH-DPIs can be observed with an increase in the proportion of MgSt in the formulations. The TH-DPIs formulated with MgSt-MSP seemed to exhibit higher ED than the other two MgSt variants, whereas the advantage of MgSt-MSP over the other two MgSt seemed to be not apparent in terms of FPF. These results suggest that the impact of homolog composition of MgSt on the aerodynamic characteristics of TH-DPIs are not very different.

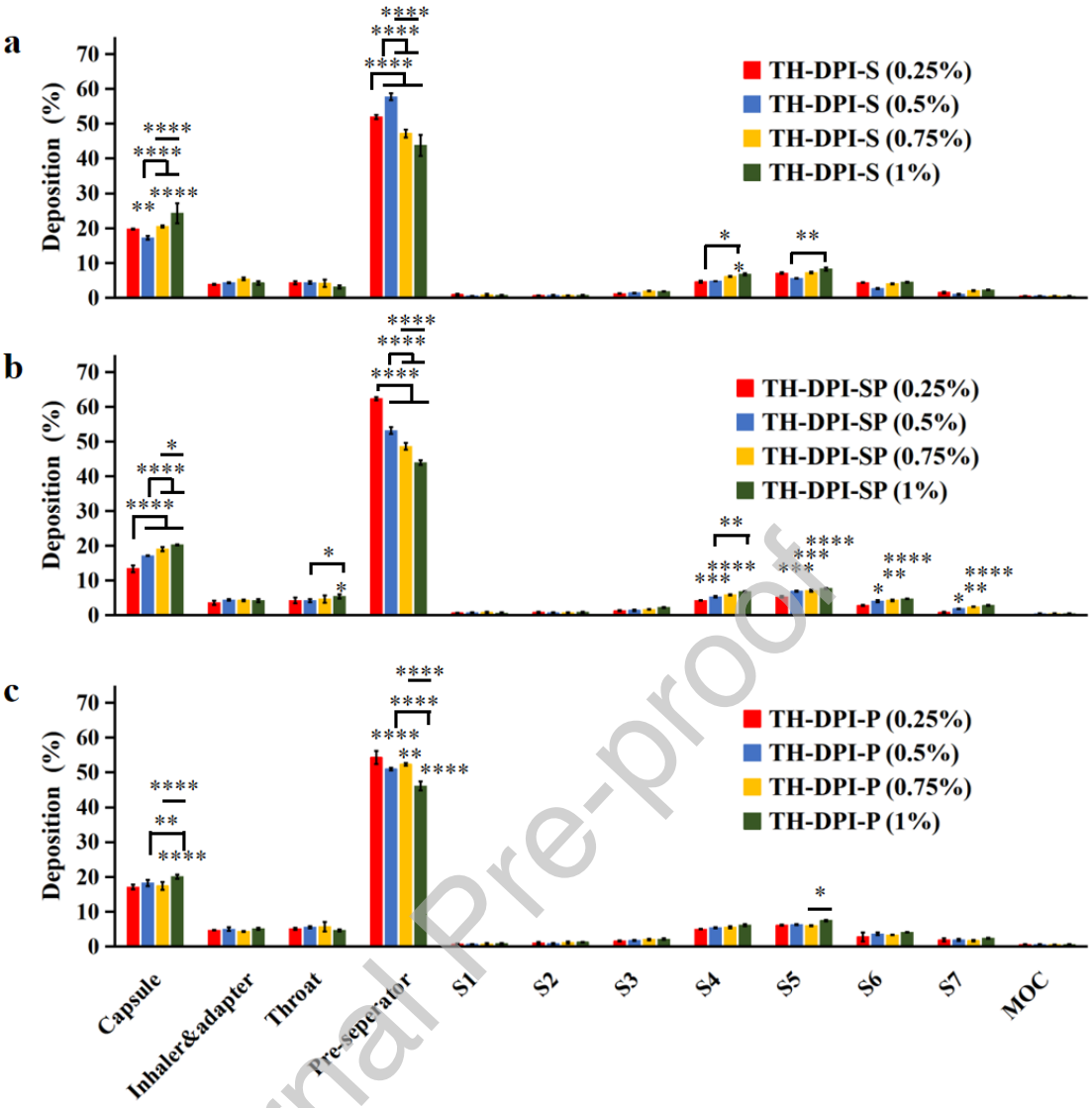

Fig. 4 Aerodynamic particle size distribution of DPIs containing different amounts of MgSt-MS (a), MgSt-MSP (b) and MgSt-MP (c). (Mean ± SD, $n = 3$). $^{*}p < 0.05$, $^{**}p < 0.01$, $^{***}p < 0.001$ and $^{****}p < 0.0001$.

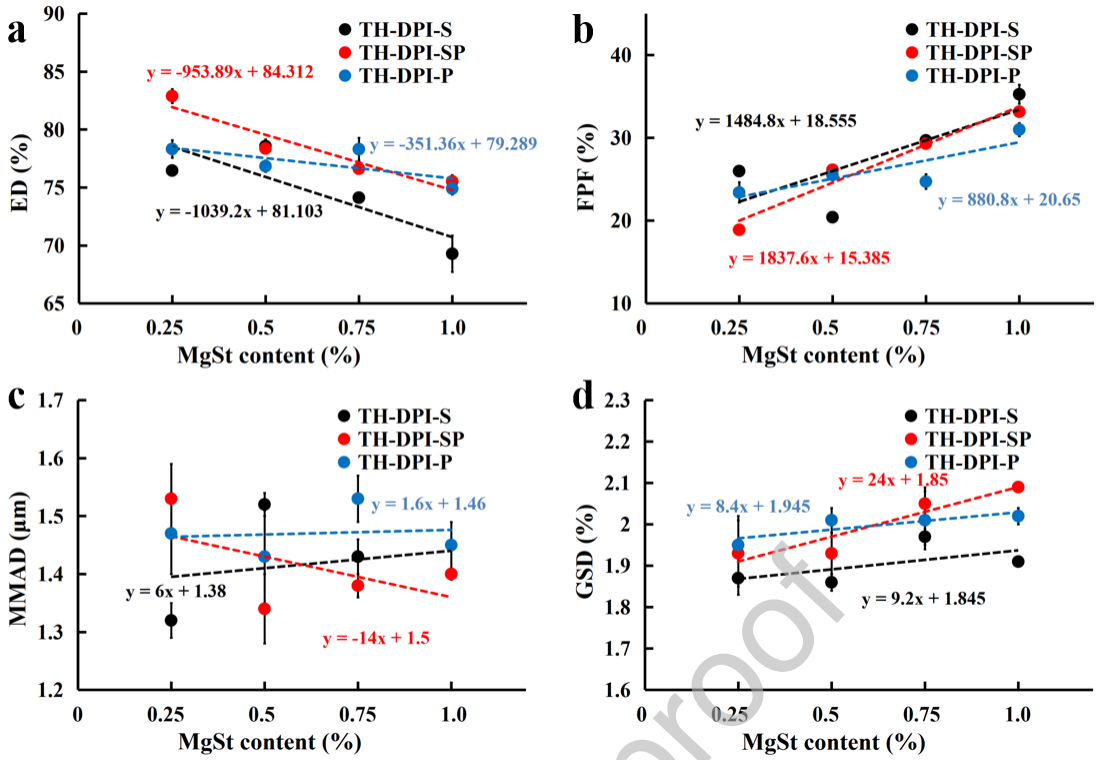

Fig. 5 ED, FPF, MMAD and GSD values of TH-DPI containing MgSt-MS, MgSt-MSP, and MgSt-MP (Mean ± SD, *n* = 3). The trend lines were represented by dashed line symbol to help the reader to identify the samples.

3.5.2 Influence of hydration state of MgSt on the aerodynamic characteristics

The deposition of TH-DPIs composed of MgSt with different hydration states in different parts of NGI are shown in Fig. 6. The results showed that different hydration states of MgSt have different effects on residual TH in the capsules and the deposition in the pre-separators. For TH-DPIs composed of MgSt-MC, the residual TH in the capsules increased with an increase in MgSt, and the deposition of TH in the pre-separator reduced with an increase in MgSt in the formulation. For TH-DPIs containing MgSt-ML, the residual TH in the capsules was generally lower than the other two MgSt variants, which were ca. 10%. However, the deposition of TH in the pre-separator are generally higher than the other two MgSt variants, which were higher than 60%. For TH-DPIs containing MgSt-MH, the residual TH in the capsules were about 20%, and the deposition of TH in the pre-separator are less than 50%.

The aerodynamic characteristics of TH-DPIs containing MgSt with different hydration states were summarized in Fig. 7. In general, TH-DPIs containing MgSt-ML exhibited higher ED, but lower FPF than TH-DPIs containing MgSt-MC or MgSt-MH. TH-DPIs containing MgSt-MH exhibited the lowest ED, but higher FPF than TH-DPIs containing MgSt-MC or MgSt-ML. The ED and FPF of TH-DPIs containing MgSt-

MC lay between those of MgSt-ML and MgSt-MH. Moreover, TH-DPIs containing MgSt-ML exhibited lower GSD as compared to the other MgSts. In terms of MMAD, TH-DPIs containing MgSt-MH exhibited smaller diameters than other two MgSt variants, which may explain they possess the highest FPF.

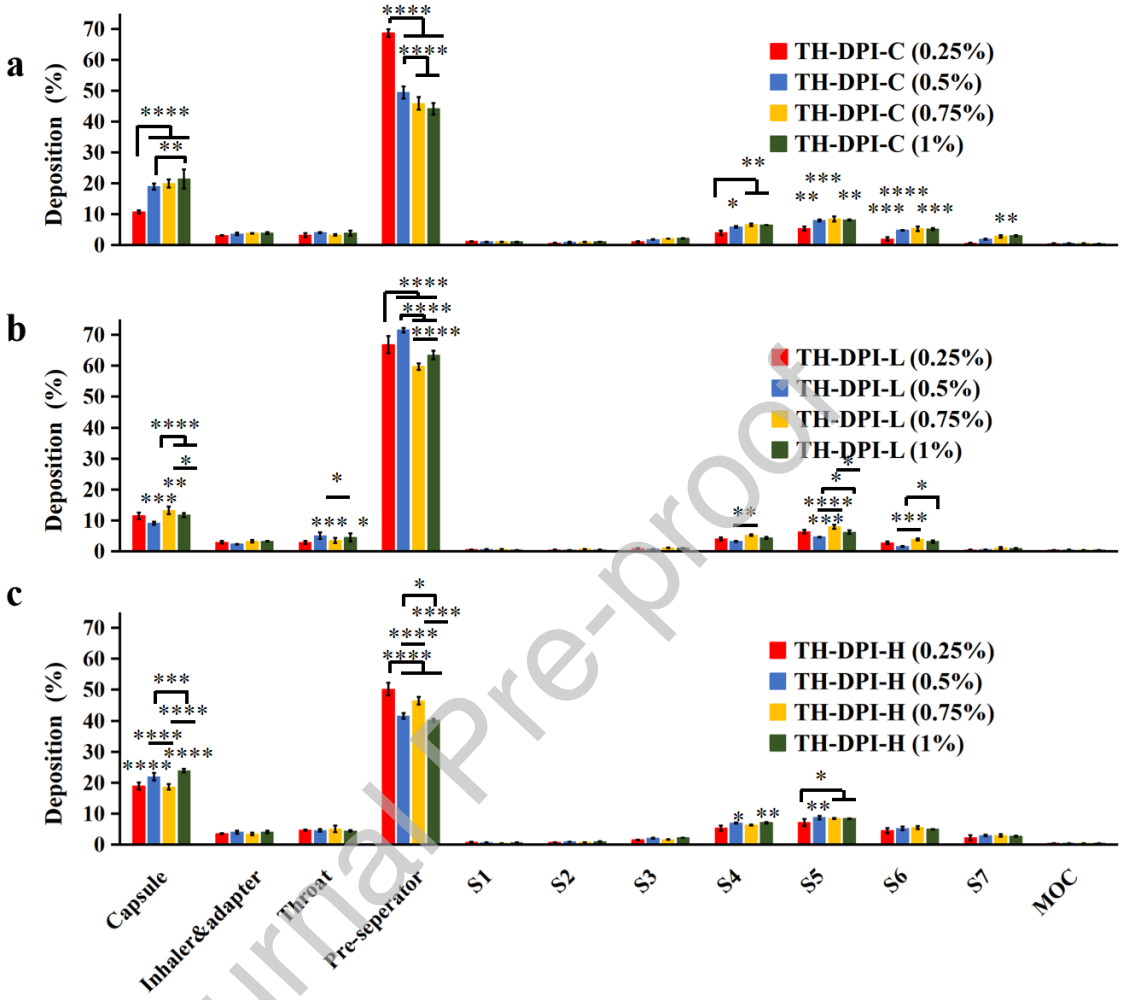

Fig. 6 Aerodynamic particle size distribution of DPIs containing different amounts of MgSt-MC (a), MgSt-ML (b) and MgSt-MH (c). (Mean ± SD, $n = 3$). $^{*}p < 0.05$, $^{**}p < 0.01$, $^{***}p < 0.001$ and $^{****}p < 0.0001$.

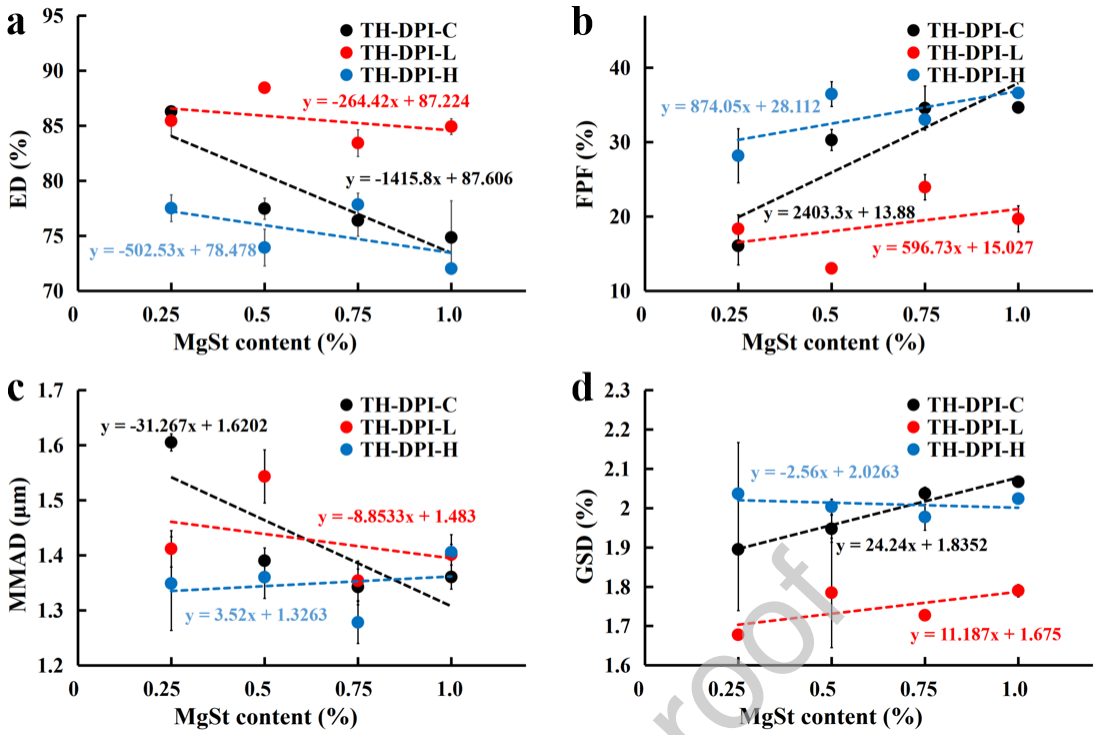

Fig. 7 ED, FPF, MMAD and GSD values of TH-DPI containing MgSt-MC, MgSt-ML and MgSt-MH. (Mean ± SD, n = 3). The trend lines were represented by dashed.

3.6. Characterization of surface energy (SE) of coarse lactose particles modified by MgSt

The NGI analyses of TH-DPIs composed of different MgSt in the section of 3.4 and 3.5 showed that the change in the hydrate state of MgSt exhibited more profound impact on the aerosol performance than the change in fatty acid composition. Usually, the addition of MgSt in carrier-based DPI formulations is believed to cover the high-energy sites on the surface of coarse lactose particles thereby facilitating detachment of fine particles from the carriers. It could be speculated that MgSt in different hydrate states might have different coating efficiency, hence the different effects on aerodynamic characteristics of the fine particles.

We attempted to characterize the surface energy of coarse lactose particles modified by using MgSt in different hydration states. As the results shown in Fig. 8A, the dispersive surface energy of coarse lactose as received was about 45 mJ/m^2. With the addition of MgSt to modify coarse lactose, the dispersive surface energy of the materials decreased. With an increase in the surface coverage (SC), the change in the dispersive surface energy was not significant though. It suggests a uniform distribution of dispersive surface energy, which could be attributed to the homogeneous adsorption ability of the carrier surface for the non-polar probe.

As shown in Fig. 8B, with an increase in SC, the specific surface energy of coarse lactose decreased. This phenomenon indicates that the defects on the surface of coarse lactose could easily combine with polar

probes. However, the specific surface energy of coarse lactose treated by MgSt under high shear mixing did not decrease, especially when the SC exceed 5%. It suggests that, under high shear mixing, the addition of MgSt could cover the defects on the surface of coarse lactose resulting in uniform distribution of specific surface energy.

The total surface energy is the contribution of both dispersive surface energy and specific surface energy. As shown in Fig. 8C, the addition of MgSt to coarse lactose could generally decrease the total surface energy. The total surface energy of coarse lactose carrier reduced from 81 mJ/m^2 to about 60 mJ/m^2 at SC of 10% after the addition of MgSt using a high shear mixing method. Interestingly, the difference in SE among coarse lactose modified by MgSt in different hydration state was small, although the coarse lactose particles modified by using MgSt-MC seem to be higher than that modified by using MgSt-ML or MgSt-MH.

The surface energy evaluation (Figure 8) demonstrate that, irrespective of hydration state, MgSt achieves widely coated on coarse lactose after high-shear blending. The fatty-acid chains of MgSt have strong lipophilicity, which can strongly repel water-based probes (ethanol and acetone) and strongly adsorb non-aqueous alkane probes. These strong adsorption and repulsion effects are manifested as insufficient sensitivity of MgSt to the adsorption amount of the probe. Therefore, we speculate that the adsorption characteristics of MgSt on the probe mask the heterogeneity of the distribution of MgSt in different hydration states on the lactose surface. Overall, although surface energy measurement confirms the widespread distribution of MgSt on lactose carriers, it cannot distinguish the surface coating differences caused by different hydration states, which is different from the obvious hydration dependence revealed by aerodynamic evaluation (Figure 6 and Figure 7).

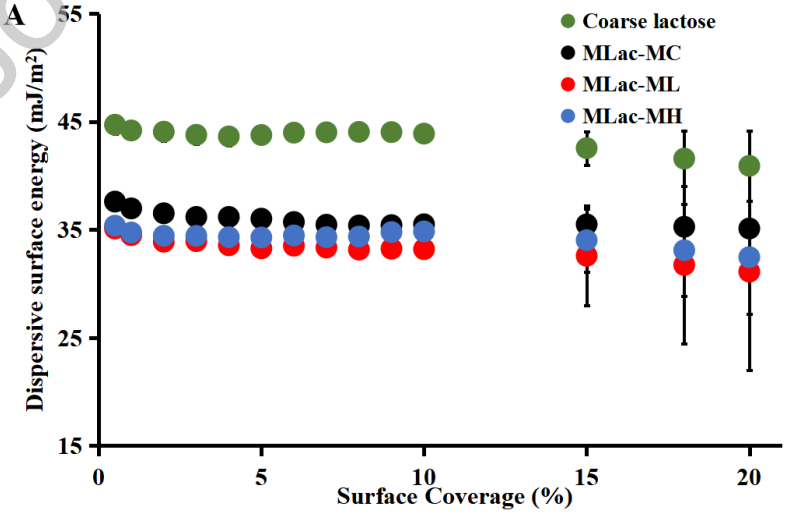

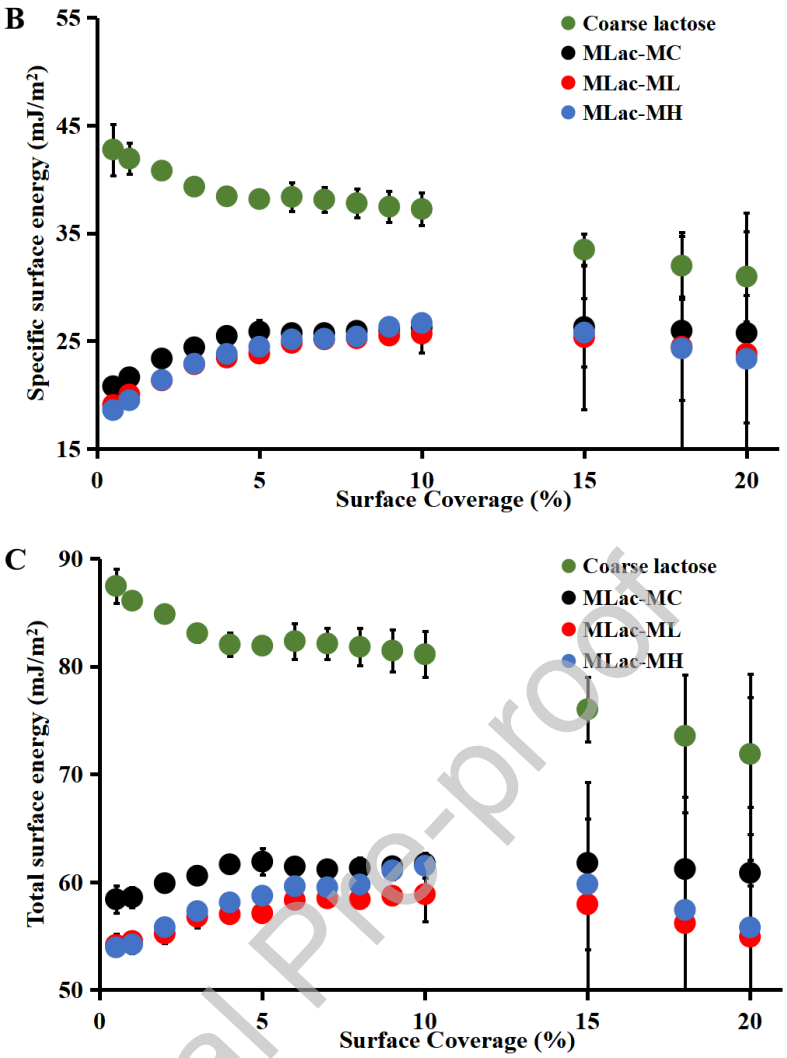

Fig. 8 Dispersive surface energy of lactose carriers (A), specific surface energy of lactose carriers (B); and total surface energy of lactose carriers (C) (Mean ± SD, n = 3).

Our research shows that the hydration state of MgSt is positively correlated with the aerodynamic properties of powder aerosols, the higher the water content in the crystalline form, the greater its modifying effect. As shown in Fig. 9, trihydrate MgSt has the largest long crystal spacing compared with dihydrate MgSt and anhydrate MgSt (Sharpe et al., 1997). During the mixing process, the collision and friction between coarse lactose particles and MgSt particles resulted in coverage of the lactose particle surfaces. Owing to the large lattice spacing, the molecular layers of trihydrate MgSt may more readily separate and spread on the surface of the coarse lactose particles, resulting in more efficient coating, thereby reducing the interaction between the fine drug particles and carriers. This observation is underpinning the importance of characterizing the solid form composition of both active substance and excipients in DPI products, as demonstrated earlier (Lee et al., 2011).

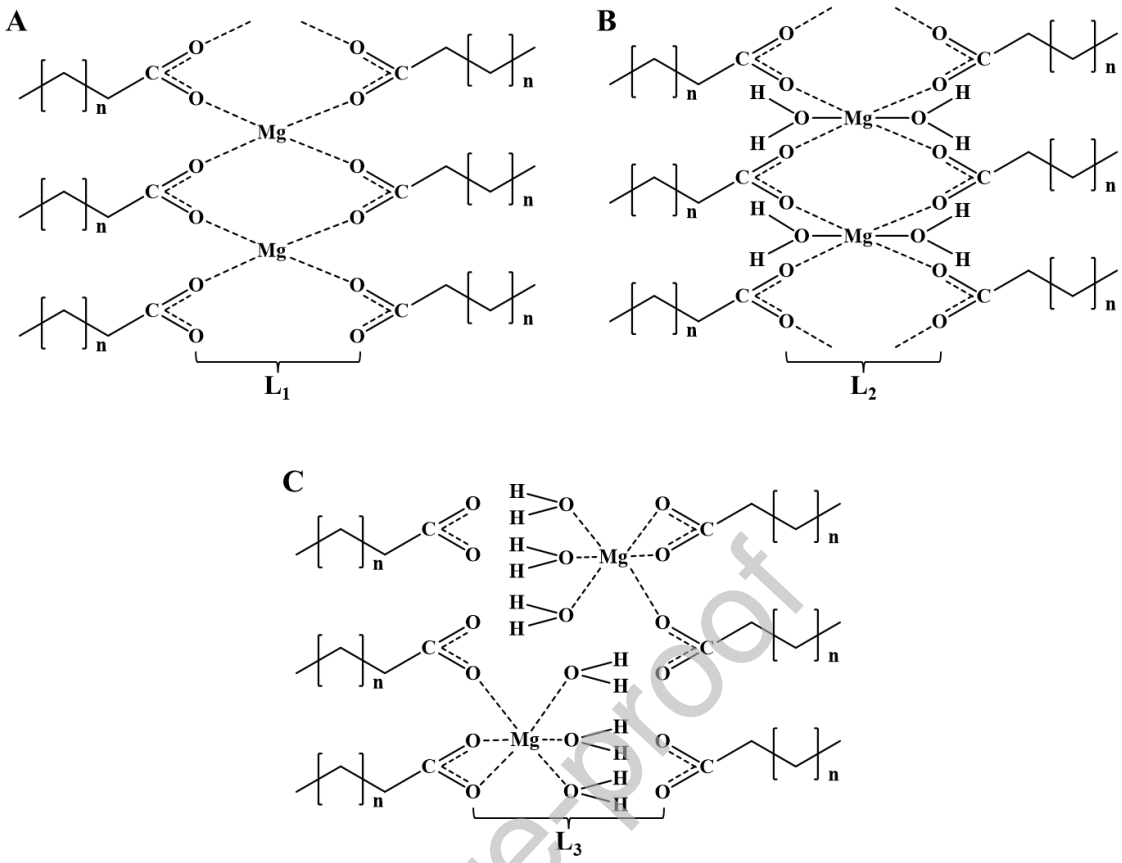

Fig. 9 Illustration of MgSt with different hydrates. A for anhydrate structure, B for dihydrate structure(Wang et al., 2019) and C for trihydrate structure (Marwaha and Rubinstein, 1988; Wang et al., 2019). (*n* = 14 or 16).

5. Conclusion

In this study, MgSt samples with different fatty acid compositions and hydration states were prepared and formulated into TH-DPIs *via* high-shear mixing. Their effects on the aerodynamic characteristics of fine particles were assessed using a Next Generation Impactor (NGI). The results showed that changes in the hydration state of MgSt exert a greater impact on DPI aerosol performance than variations in fatty acid composition. No significant differences in aerodynamic characteristics were observed among TH-DPIs when the fatty acid composition of MgSt was varied. By contrast, formulations containing trihydrate MgSt exhibited better aerosol performance than those containing dihydrate or MgSt with lower hydration state. This improved performance of trihydrate MgSt may be attributed to its larger lattice spacing, which could facilitate coating on the carrier surface during high-shear mixing and thereby promote detachment of fine particles from the carriers during inhalation.

6. Acknowledgements

This work was financially supported by the National Major Scientific and Technological Special Project for "Significant New Drug Development" of China (No. 2018ZX09739009), the Liaoning Pan Deng Xue Zhe Scholar (No. XLYC2002061), and the Overseas Expertise Introduction Project for Discipline Innovation ("111 Project") (No. D20029). We would like to thank Prof. Regina Scherließ for providing the access to IGC measurement. T.L. would like to thank the China Scholarship Council (No. 201908210308) and NordForsk for the Nordic University Hub project #85352 (Nordic POP, Patient Oriented Products) for financial support. D.C. acknowledges financial support from the Guiding Project for Science and Technology of Liaoning Province (No. 2019-ZD-0448), and Ministry of Education Chunhui Program (2020).

References

Begat, P., Morton, D., Staniforth, J.N., Price, R., 2004. The cohesive-adhesive balances in dry powder inhaler formulations I: Direct quantification by atomic force microscopy. Pharm. Res. 21, 1591–1597.

Begat, P., Price, R., Harris, H., Morton, D., Staniforth, J.N., 2005. The Influence of Force Control Agents on the Cohesive-Adhesive Balance in Dry Powder Inhaler Formulations. KONA Powder and Particle Journal 23, 109–121.

Boer, A.H.D., Hagedoorn, P., Hoppentocht, M., Buttini, F., Grasmeijer, F., Frijlink, H.W., 2017. Dry powder inhalation: past, present and future. Expert Opinion on Drug Delivery 14, 499–512.

Brunauer, S., Emmett, P.H., Teller, E., 1938. Adsorption of Gases in Multimolecular Layers. J. Am. Chem. Soc. 60, 309–319. https://doi.org/10.1021/ja01269a023

Calahan, J.L., Paul, S., Yanez, E.G., Deneve, D., Munson, E.J., 2020. The impact of solid-state form, water content and surface area of magnesium stearate on lubrication efficiency, tabletability, and dissolution. Pharmaceutical Development and Technology 26, 1–7.

Delaney, S.P., Nethercott, M.J., Mays, C.J., Winquist, N.T., D Arthur, Calahan, J.L., Sethi, M., Pardue, D.S., Kim, J., Amidon, G., 2017. Characterization of Synthesized and Commercial Forms of Magnesium Stearate Using Differential Scanning Calorimetry, Thermogravimetric Analysis, Powder X-Ray Diffraction, and Solid-State NMR Spectroscopy. J. Pharm. Sci. 106, 338–347.

Ertel, K.D., Carstensen, J.T., 1988. Chemical, Physical, and Lubricant Properties of Magnesium Stearate. Journal of Pharmaceutical Sciences 77, 625–629. https://doi.org/10.1002/jps.2600770715

Guchardi, R., Frei, M., John, E., Kaerger, J.S., 2008. Influence of fine lactose and magnesium stearate on low dose dry powder inhaler formulations. Int. J. Pharm. 348, 10–7. https://doi.org/10.1016/j.ijpharm.2007.06.041

Herzberg, M., Rekis, T., Støttrup Larsen, A., Gonzalez, A., Rantanen, J., Østergaard Madsen, A., 2023. The structure of magnesium stearate trihydrate determined from a micrometre-sized single crystal using a microfocused synchrotron X-ray beam. Acta Crystallogr B Struct Sci Cryst Eng Mater 79, 330–335. https://doi.org/10.1107/S2052520623005607

Jetzer, M., Schneider, M., Morrical, B., Imanidis, G., 2017. Investigations on the Mechanism of Magnesium Stearate to Modify Aerosol Performance in Dry Powder Inhaled Formulations. J. Pharm. Sci. 107, 984–998.

Kong, L., Zhao, Y., Wang, Y., Chang, X., Cui, L., Gu, G., Ma, Z., Lu, Q., Zhou, L., Ding, L., Wang, Z., Shao, Y., Tang, H., Zhang, C., Hui, F., Mei, X., Xin, J., Huo, J., Sun, S., Zhu, S., Yao, C., Du, G., Cheng, M., Kang, J., 2021. Efficacy and safety of tratinterol hydrochloride tablets in bronchial asthma: a randomized double-blind and multicenter clinical trial. Journal of Asthma 58, 85–92. https://doi.org/10.1080/02770903.2019.1663427

Lau, M., Young, P.M., Traini, D., 2017. Co-milled API-lactose systems for inhalation therapy: impact of magnesium stearate on physico-chemical stability and aerosolization performance. Drug Dev. Ind. Pharm. 43, 980–988. https://doi.org/10.1080/03639045.2017.1287719

Lee, Y.Y., Wu, J.X., Yang, M., Young, P.M., Berg, F.V.D., Rantanen, J., 2011. Particle size dependence of polymorphism in spray-dried mannitol. European Journal of Pharmaceutical Sciences 44, 41–48.

Liu, T., Tong, S., Liao, Q., Pan, L., Cheng, M., Rantanen, J., Cun, D., Yang, M., 2023. Role of dispersion enhancer selection in the development of novel tratinterol hydrochloride dry powder inhalation formulations. International Journal of Pharmaceutics 635, 122702. https://doi.org/10.1016/j.ijpharm.2023.122702

Liu, T., Tong, S., Liao, Q., Pan, L., Cheng, M., Rantanen, J., Cun, D., Yang, M., 2022. Role of Dispersion Enhancer Selection in the Development of Novel Tratinterol Hydrochloride Dry Powder Inhalation Formulations. SSRN Journal. https://doi.org/10.2139/ssrn.4176020

Marwaha, S.B., Rubinstein, M.H., 1988. Structure-lubricity evaluation of magnesium stearate. International Journal of Pharmaceutics 43, 249–255. https://doi.org/10.1016/0378-5173(88)90281-5

Ooi, J., Traini, D., Hoe, S., Wong, W., Young, P.M., 2011. Does carrier size matter? A fundamental study of drug aerosolisation from carrier based dry powder inhalation systems. Int. J. Pharm. 413, 1–9.

https://doi.org/10.1016/j.ijpharm.2011.04.002

Peng, T., Lin, S., Niu, B., Wang, X., Huang, Y., Zhang, X., Li, G., Pan, X., Wu, C., 2016. Influence of physical properties of carrier on the performance of dry powder inhalers. Acta Pharmaceutica Sinica B 11.

Pilcer, G., Wauthoz, N., Amighi, K., 2012. Lactose characteristics and the generation of the aerosol. Adv Drug Deliv Rev 64, 233–256. https://doi.org/10.1016/j.addr.2011.05.003

Sharpe, S.A., Celik, M., Newman, A.W., Brittain, H.G., 1997. Physical characterization of the polymorphic variations of magnesium stearate and magnesium palmitate hydrate species. Struct. Chem. 73–84.

Swaminathan, V., Kildsig, D.O., 2001. An examination of the moisture sorption characteristics of commercial magnesium stearate. AAPS PharmSciTech 2, 73–79.

Wang, T., Potts, A.R., Hoag, S.W., 2019. Elucidating the Variability of Magnesium Stearate and the Correlations With Its Spectroscopic Features. Journal of Pharmaceutical Sciences 108, 1569–1580. https://doi.org/10.1016/j.xphs.2018.11.041

Xian, M.Z., Martin, G.P., Marriott, C., Pritchard, J., 2000. The influence of carrier morphology on drug delivery by dry powder inhalers. Int. J. Pharm. 200, 93–106.

Zhou, Q., Qu, L., Gengenbach, T., Larson, I., Stewart, P.J., Morton, D.A.V., 2012. Effect of Surface Coating with Magnesium Stearate via Mechanical Dry Powder Coating Approach on the Aerosol Performance of Micronized Drug Powders from Dry Powder Inhalers. AAPS PharmSciTech 14, 38–44. https://doi.org/10.1208/s12249-012-9895-z

Graphical abstract